A Study of Nickel Electrodeposition on Paraffin-Impregnated Graphite Electrode

by **Magdaléna Strečková**[a]), **Renáta Oriňáková**[*a]), **Roland Rozik**[b]), **Libuše Trnková**[b]), and **Miriam Gálová**[a])

[a]) Institute of Chemistry, Faculty of Science, P. J. Šafárik University, Moyzesova 11, 041 54 Košice, Slovak Republic (phone: +421-55-6222605; fax: +421-55-6222124; e-mail: renata.orinakova@upjs.sk)
[b]) Department of Physical and Theoretical Chemistry, Faculty of Science, Masaryk University, Kotlářská 2, 611 37 Brno, Czech Republic

The aim of the present work was to elucidate the mechanism of electrolytic deposition of Ni on paraffin-impregnated graphite electrode (PIGE). This process is influenced by H_2 evolution, which occurs in the same potential region. On the basis of the results obtained by linear and cyclic voltammetry, elimination voltammetry with linear scan (EVLS) was used to evaluate both processes. H_2 Evolution alone was studied in sulfate supporting electrolyte, and the previously suggested mechanism for this process according to *Volmer–Heyrovsky* was confirmed by EVLS. It was found that both the Ni^{2+} concentration and pH affect the polarization behavior of PIGE significantly. Two separated cathodic peaks were observed at low Ni^{2+} and high H^+ concentrations, and the separation was better at higher scan rates. EVLS confirmed the most-probable mechanism of Ni deposition as being controlled by slow transfer of the first electron under formation of $[NiOH]^+$ as an intermediate. EVLS also indicated slow reduction of H^+ preceding the reduction of Ni^{2+}. The same was confirmed by studying the anodic dissolution at different switching potentials. The results were complemented by scanning electron microscopy (SEM).

Introduction. – Electrodeposition of nickel (Ni) and its alloys on various less-noble surfaces from *Watts* electrolyte containing both sulfate and chloride ions is a widely used technique for improving the mechanical and chemical properties of plated surfaces. During recent years, electroplating from mixed electrolytes has become most widespread in metallurgy industry. However, why exactly this electrolyte composition is so convenient, remains a challenging question. Without a detailed study in the two separate electrolytes (chloride and sulfate bath), as well as in the presence and/or absence of boric acid, the elucidation of the Ni-reduction mechanism from complete *Watts* electrolyte is a very difficult task. Several studies have addressed different aspects of Ni electrodeposition in the two above-mentioned electrolyte systems [1–5].

One of the main components of *Watts* bath is boric acid [6][7]. Our previous studies confirmed that the presence of boric acid alters the polarization behavior of Ni reduction from the two above-mentioned electrolytes [8][9]. Moreover, higher-quality deposit has been obtained when boric acid was used in chloride solution [8–12]. The evolution of H_2 is another important effect occurring during Ni electrodeposition. The great affinity between H_2 and Ni facilitates the adsorption step on the Ni surface, probably due to the formation of the activated complex $[Ni{-}H{\cdots}H{\cdots}OH]^{\neq}$. Hence, the *Heyrovsky* electrochemical-desorption step seems most likely to be rate determining [13].

In our previous work, the influence of pH on Ni electrodeposition in the chloride supporting electrolyte was studied [9]. Preliminary experimental results showed different polarization behavior of Ni reduction on paraffin-impregnated graphite electrode (PIGE) from chloride and sulfate baths. Significant differences were already registered by voltammetric measurements of individual supporting electrolytes. Electrodeposition of Ni from chloride bath (pH 2) is manifested by a single voltammetric peak [8].

The present work shows that electrolytic deposition of Ni from sulfate electrolyte is more complicated than expected, and proceeds by a different mechanism compared to deposition from chloride electrolyte. The main aim of this work is to elucidate the mechanism of Ni electrodeposition on PIGE from the sulfate supporting electrolyte, without addition of boric acid, and to evaluate the linear sweep and cyclic-voltammetric results using elimination voltammetry with linear scan (EVLS). Thereby, PIGE was used because of the good reproducibility of its surface, in contrast to some metallic electrodes, as well as due to further advantages such as *1*) simple preparation, *2*) easy surface renewal, and *3*) reasonable price.

The EVLS technique was used to achieve a better understanding of the electrodeposition mechanism. We expected that EVLS is capable to trace some partial processes of the Ni reduction on PIGE hidden in voltammetric responses, and to facilitate the resolution of interconnected processes. This technique has been described very precisely before [8][14–18], where the theoretical derivation of elimination equations, their explanation, and experimental verification can be found. In addition, some necessary conditions of EVLS will be listed below. The general idea is based on the elimination of particular currents (*e.g.*, kinetic, diffusion, and charging currents I_k, I_d, and I_c, resp.) by means of a linear combination of the total current measured at different scan rates. This linear combination is termed 'elimination function', $f(I)$. Therefore, EVLS can be considered as the mathematical processing of voltammetric signals in which two necessary conditions must be fulfilled: *1*) the total current I is the sum of the particular currents, and *2*) the particular currents eliminated are expressed as a product of the scan-rate and electrode-potential functions [14].

In this work, the elimination functions *E1* (elimination of I_k, conservation of I_d, and distortion of I_c) and *E4* (simultaneous elimination of I_k and I_c, conservation of I_d) were chosen. While the calculation of *E4* coefficients was published in previous papers [14][15][18], the calculation of *E1* coefficients is shown here. For a total current measured at a reference scan rate (total current I) and at half reference scan rate ($I_{1/2}$), we can write:

$$I_{1/2} = (I_d)_{1/2} + (I_k)_{1/2} \quad \text{or} \quad a_1 I_{1/2} = \boxed{a_1 \sqrt{\frac{1}{2}} I_d} + \boxed{a_1 I_k} \tag{1}$$

$$I = I_d + I_k \quad \text{or} \quad a_2 I = \underset{\downarrow}{\boxed{a_2 I_d}} + \underset{\downarrow}{\boxed{a_2 I_k}} \tag{2}$$

$$I_d \qquad 0$$

According to this requirement, it follows:

$$a_1 \sqrt{\frac{1}{2}} I_d + a_2 I_d = I_d \tag{3}$$

$$a_1 I_k +_2 I_k = 0 \tag{4}$$

$$a_1 = -3.4142, \quad a_2 = 3.4142 \tag{5}$$

The corresponding elimination function is:

$$f(I) = 3.4142\ I - 3.4142\ I_{1/2} \tag{6}$$

In *E1*, the charging current I_c is distorted by the parameter κ:

$$\frac{1}{2}\ a_1 I_c + a_2 I_c = \kappa\ I_c \tag{7}$$

$$\frac{1}{2}\ a_1 + a_2 = \kappa \tag{8}$$

and with *Eqn. 5*, we can calculate this parameter as $\kappa = 1.707$.

The derivation of the second elimination function, *E4*, is similar, however, the currents eliminated are now I_k and I_c, with I_d being conserved, which results in:

$$f(I) = 17.485\ I - 11.657\ I_{1/2} - 5.8284\ I_2 \tag{9}$$

In *Eqn. 9*, I is the total voltammetric current measured at the so-called reference scan rate, and $I_{1/2}$ and I_2 are the voltammetric currents measured at half and double values of the reference scan rate, respectively.

Experimental. – Cyclic and linear-sweep voltammetric measurements were used to verify the influence of different experimental conditions on Ni deposition. Electrochemical measurements were carried out in potentiostatic regime with a conventional three-electrode cell thermostated at 24°. As a working electrode, PIGE was used, and mechanically renewed with emery paper, polished with glossy paper, and rinsed with redistilled H_2O before each experiment. The reference electrode was Ag/AgCl/3M KCl, and the auxiliary electrode was a Pt wire. The reference electrode was separated from the cell by a salt bridge containing the supporting electrolyte. All voltammetric curves were recorded with a potential step of 2 mV at three different scan rates: 12.5, 25, and 50 mV/s. The 25-mV/s data were used in EVLS as the reference scan rate. Cathodic-linear-polarization curves were evaluated using EVLS.

Electrolytes of the following composition were investigated: 0.5M Na_2SO_4 (supporting electrolyte), and 0.5M Na_2SO_4 containing 1–100 mM $NiSO_4$. All originally prepared electrolytes were adjusted to the required pH by addition of H_2SO_4. The surface character of the deposited Ni coatings was examined with a *Tesla BS-340* scanning-electron microscope (SEM).

Results and Discussion. – 1. *Sulfate Supporting Electrolyte*. The effect of pH on the voltammetric curves of 0.5M Na_2SO_4 at a scan rate of 25 mV/s is shown in *Fig. 1*. The reduction signals were attributed to the reduction of H_2. The highest cathodic peak and the onset of reduction at the most-positive potential were detected at pH 2. An increase in pH caused a decrease of the peak height, and at pH 4, only a negligible signal was observed.

The voltammogram of the sulfate electrolyte at pH 2 exhibited one reduction peak at *ca.* −1400 mV, which was shifted to more-negative potentials when the scan rate was

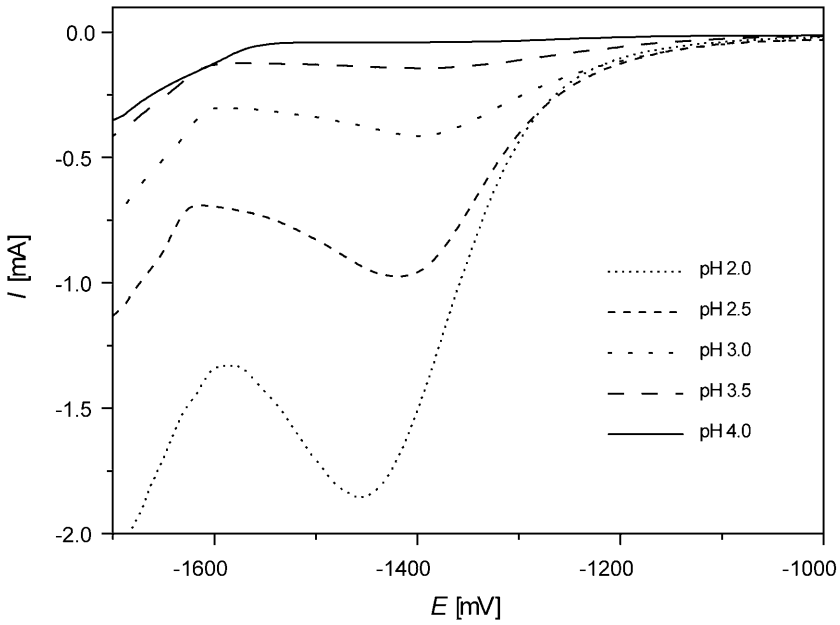

Fig. 1. *Voltammetric signals for 0.5*M Na_2SO_4 *as Supporting Electrolyte on PIGE*. Conditions: reference electrode, Ag/AgCl/3M KCl; potential step, 2 mV; scan rate, 25 mV/s. The pH was adjusted with H_2SO_4.

increased (*Fig. 2,a*). The dependence of the height of the reduction peak on the scan rate was analyzed according to the *Delahay* equation [19]. The nearly diffusion character of the process at peak potential was evident from a slope of 0.45 of the plot of log *I* *vs.* log *v*. The diffusion character of the process at sufficiently negative potentials was confirmed also by elimination voltammetry (*Fig. 2,b*).

The elimination procedure transforms the irreversible current in a special way [14], which results in an increase of peak height, and in a decrease of peak width. In comparison with original voltammetric peaks, the EVLS peaks were 4.4- and 11.2-times higher for *E1* and *E4*, respectively. This increase is also applicable in electroanalysis. The observed voltammetric behavior was examined by means of the elimination functions *E1* and *E4* according to the method suggested in reference [18]. The parallel course of the elimination functions *E1* and *E4* at the onset of the reduction process indicates kinetic control (see left part of the insert in *Fig. 2,b*). This kinetic control (I_{pp}) is probably caused by inhibition of the first electron transfer (*Eqn. 10*) in the overall process. At more-negative potentials, the process is controlled by diffusion of H_3O^+ to the electrode surface. The reduction process runs *via* reaction of the adsorbed H_2 with hydroxonium ions from the solution (*Eqn. 11*), which results in the formation of H_2 molecules and, subsequently, their desorption (*Eqn. 12*):

$$\text{at more-positive potentials: } M + H_3O^+ + e^- \rightarrow MH_{ads} + H_2O \quad (10)$$

$$\text{at more-negative potentials: } MH_{ads} + H_3O^+ + e^- \rightarrow M + H_2 + H_2O \quad (11)$$

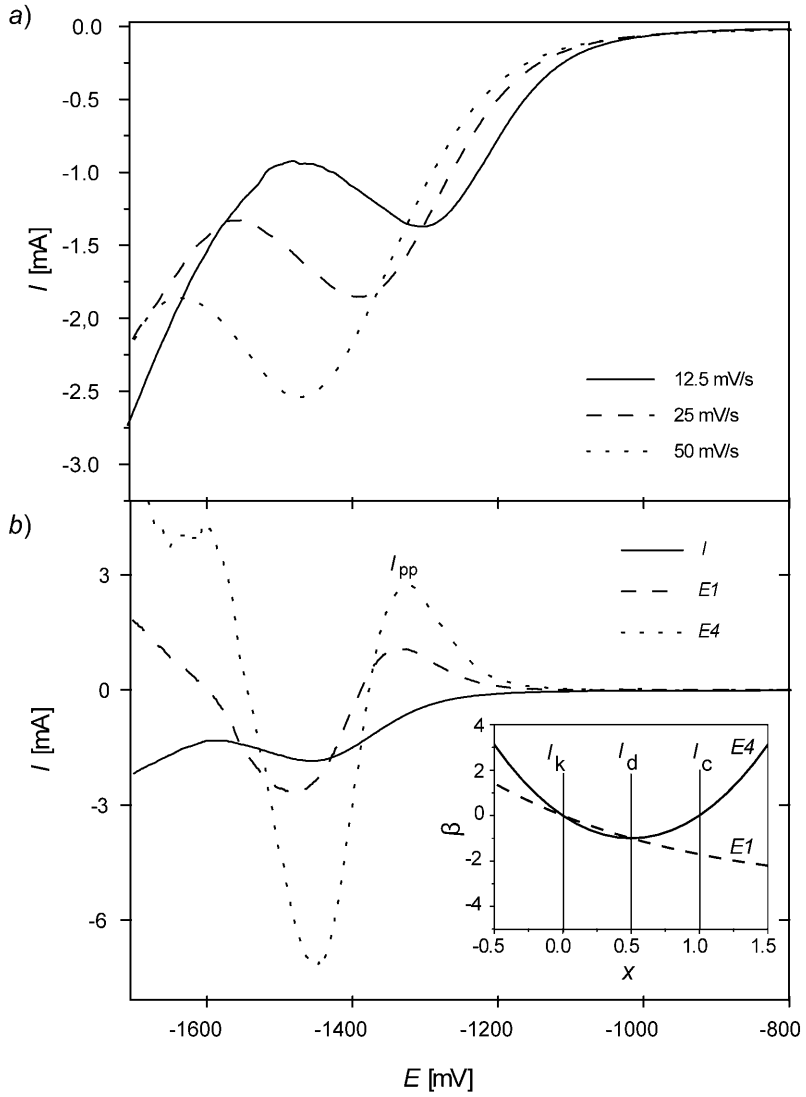

Fig. 2. a) *Cathodic cyclic voltammograms at different scan rates on PIGE*. Conditions: supporting electrolyte, 0.5M Na_2SO_4, pH 2.0 (H_2SO_4); potential step, 2mV. b) *Corresponding Elimination voltammetric curves*. Experimental conditions as in *Fig. 1*. *E1* is the function eliminating the kinetic current and conserving the diffusion current (the charging current is distorted). *E4* is the function eliminating the kinetic and charging currents, but conserving the diffusion current. Insert: dependence of elimination-current coefficient β on scan rate coefficient x for *E1* and *E4*.

$$n\ H_2 \rightarrow (H_2)_n \tag{12}$$

Here, M stands for the metal surface of the PIGE electrode. The suggested mechanism of H_2 reduction is one of the generally accepted mechanisms of hydrogen over-

potential in aqueous solutions, as analyzed in detail, *e.g.*, in [19–22]. *Tafel* coefficients calculated from $\eta = a + b \log i$ were $b = -0.1517$ and $a = -1.809$ (where η is the overpotential, and i is the current density). The value of b indicates that the transfer of the second electron on PIGE proceeds according to *Eqn. 11* [22].

2. *Reduction of Ni^{2+}.* The Ni electrodeposition from sulfate supporting electrolyte at pH 2 and 4 was investigated. A strong influence of H_2 evolution was observed in this electrolyte in an identical potential range in all experiments. Two clear reduction peaks, denoted as *A* and *B*, were observed at conditions indicating excess of H_3O^+ over Ni^{2+}, *e.g.*, at pH 2 and low Ni^{2+} concentration (*Fig. 3*). With increasing Ni^{2+} concentration, both cathodic peaks merged, and above 100 mM Ni^{2+}, only one reduction signal was detected. The peak height did not increase proportionally to the concentration increase in Ni^{2+}. A plot of the current *I vs.* $[Ni^{2+}]$ is depicted in the insert of *Fig. 3*, and clearly shows the presence of adsorption of some of the Ni particles participating in the electrode process.

The best separation of the two reduction peaks was achieved at higher scan rate (50 mV/s; *Fig. 4,a*). According to the *Delahay* equation [19], the scan-rate coefficients were calculated for both cathodic processes, and the values for peaks *A* and *B* were found to be 0.47 and 0.43, respectively. Thus, the diffusion character of peak *A* was more significant.

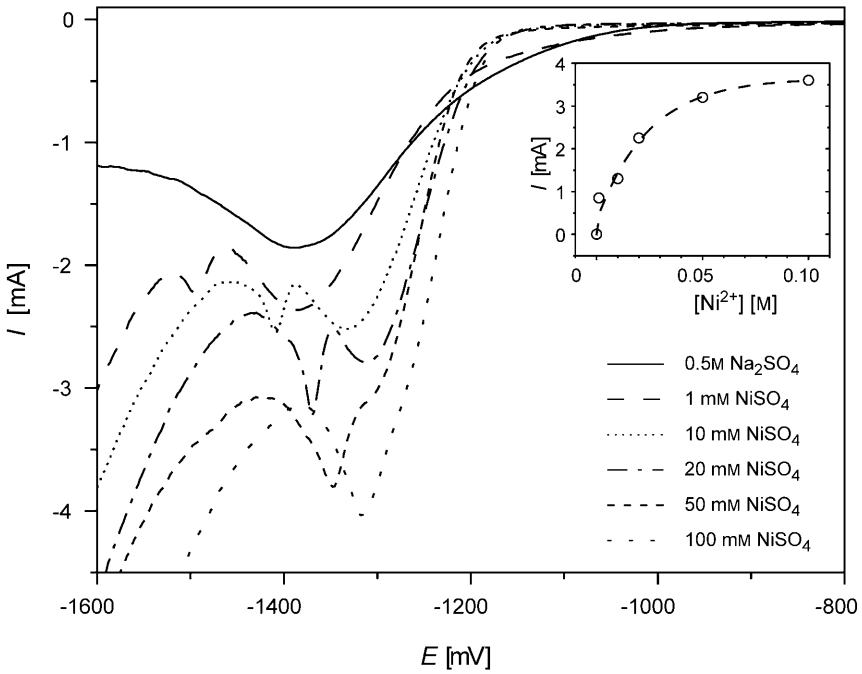

Fig. 3. *Cathodic cyclic voltammograms for nickel reduction on PIGE as a function of the concentration of $NiSO_4$.* Supporting electrolyte, 0.5M Na_2SO_4, pH 2.0 (H_2SO_4); scan rate, 25 mV/s; other conditions as in *Fig. 1*. Insert: dependence of the total current *I* on $[Ni^{2+}]$, calculated as the sum of currents of peaks *A* and *B* for each Ni^{2+} concentration (see text).

The above conclusion was further corroborated by the results of EVLS. The elimination functions *E1* and *E4* (*Fig. 4*, *b*) were in agreement with a kinetically controlled process at the onset of both cathodic waves. However, at more-negative potentials, the process was controlled by diffusion. By quantification of the kinetics (I_{pp} values) obtained in supporting and in Ni-containing electrolytes, similar values of I_{pp} in *E4* were obtained (*Table*).

The above results confirmed that, under given conditions [supporting or Ni-containing electrolyte, pH 2, low Ni concentration (up to 10 mM)], the same step is rate deter-

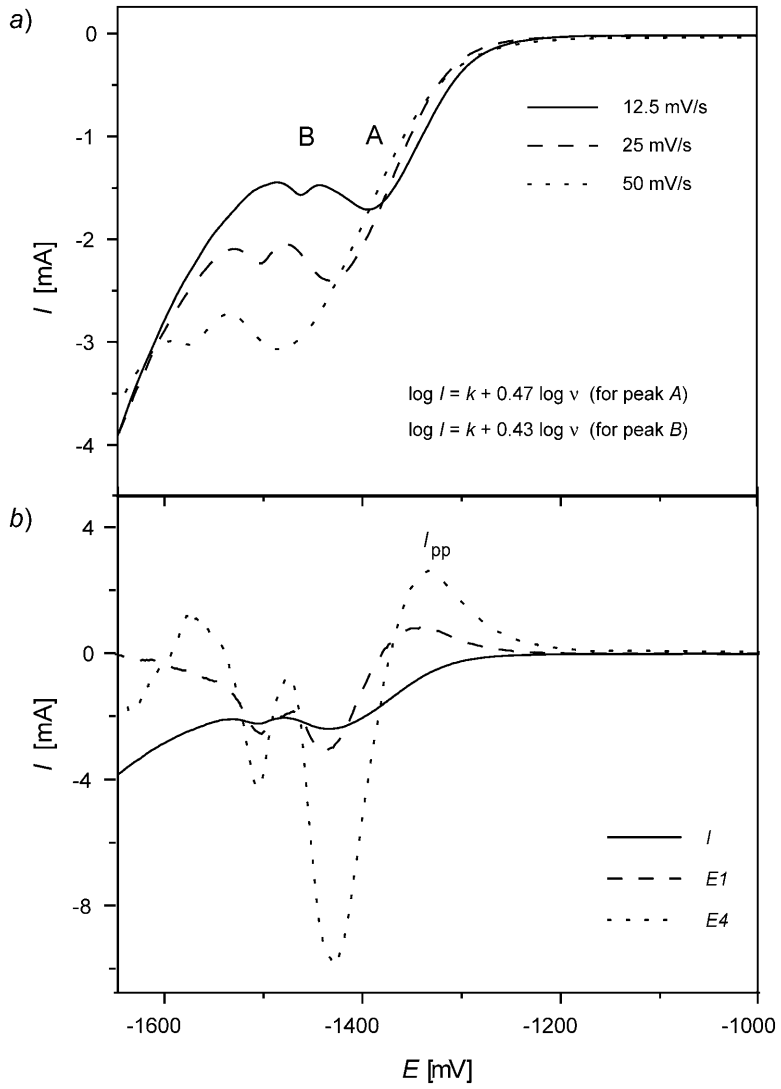

Fig. 4. a) *Cathodic voltammetric curves of 1mM $NiSO_4$* (pH 2.0) *at different scan rates.* Other experimental conditions as in *Fig. 1*. b) *Corresponding* E1 *and* E4 *elimination voltammograms*

Table. *Values of* I_{pp} *in the Elimination Function* E4 *at Different Nickel Concentrations.* In 0.5M Na_2SO_4 electrolyte; the pH was adjusted with H_2SO_4.

$[Ni^{2+}]$ [mM]	I_{pp} [mA]	
	pH 2.0	pH 4.0
0	3.20	0[a])
1	3.25	1.72
2	–	2.42
10	3.92	3.90
50	10.51	–
100	–	15.20

[a]) No signal.

mining. The transfer of the first electron, corresponding to H_2 evolution (*Eqn. 10*), is the kinetically controlled slow process also in the case of Ni reduction. The highest values of I_{pp} were achieved in electrolytes with high concentration of Ni^{2+}.

Up to now, several mechanisms of Ni deposition from Ni-plating electrolytes have been suggested. In general, two one-electron transfer steps of metal reduction have been assumed [13][23]:

$$Ni^{2+} + H_2O \rightleftharpoons Ni(OH)^+ + H^+ \tag{13}$$

$$Ni(OH)^+ + e^- \rightarrow [Ni(OH)]_{ads} \tag{14}$$

$$[Ni(OH)]_{ads} + e^- \rightarrow Ni + OH^- \tag{15}$$

where $Ni(OH)_{ads}$ stands for the active intermediate. Our results indicate, however, that the slow step (*Eqn. 10*) in H_2 reduction proceeds simultaneously with the reduction of the Ni^{2+} species. Evolution of H_2 causes alkalization in the vicinity of the electrolyte and, thus, facilitates the formation of the electroactive particle ($[NiOH]^+$). The diffusion character of the more-positive peak (*A*) can, most likely, be ascribed to a diffusion-controlled transport of Ni^{2+} species to the electrode in the peak-potential region.

To clarify the suggested sequence of processes and to identify the intermediates and products giving rise to the cathodic peaks, the anodic scan was studied (*Fig. 5*). The experiments showed anodic dissolution of Ni deposit from 0.5M Na_2SO_4/1 mM $NiSO_4$ (pH 2) at a scan rate of 25 mV/s. The Ni deposition was carried out on PIGE in potentiostatic regime at different potentials (*Fig. 5*, *a*), and at a deposition time of 10 min. Under the given experimental conditions, the current started to increase at *ca.* -1000 mV, but no observable Ni deposit was detected. The first fraction of the deposited Ni was detected anodically only at -1142 mV (insert in *Fig. 5*, *b*). This observation supports the above assumption that the current at the onset of the overall deposition process is, to a major extent, consumed by the H_2 reduction. However, the highest anodic signal was recorded in the case of the deposit obtained at a potential of -1360 mV, which is nearly the maximum of the first reduction peak. A wide anodic peak was registered during oxidation of the deposit formed at -1460 mV, which is the minimum

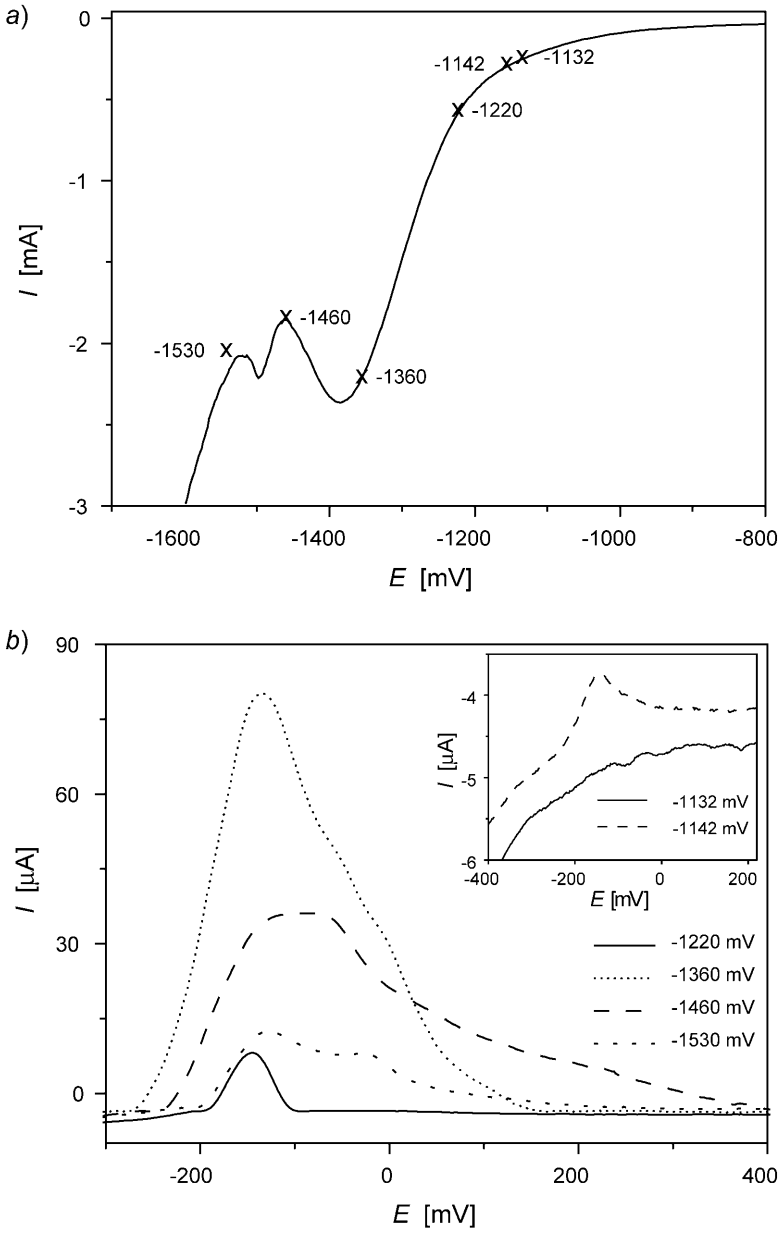

Fig. 5. a) *Cathodic cyclic voltammogram of the nickel reduction from 0.5*M Na_2SO_4 *containing 1 m*M $NiSO_4$ (pH 2.0). Potentials selected for dissolution are indicated. Deposition time, 10 min. b) *Corresponding anodic dissolution of Ni deposit on PIGE* (conditions as in *a*).

between the two cathodic peaks. The current in the whole region was lower. The decrease in the dissolved Ni content from this deposit is probably caused by the high catalytic activity of freshly deposited Ni towards H_2 evolution. When the deposition potential was shifted to even more-negative values (−1530 mV), two distinct anodic peaks were detected.

Ni deposits are known to often contain two phases (α and β) of Ni/H solid solution [23–25]. The peak at more-negative potential (peak *B*) is likely to correspond to the

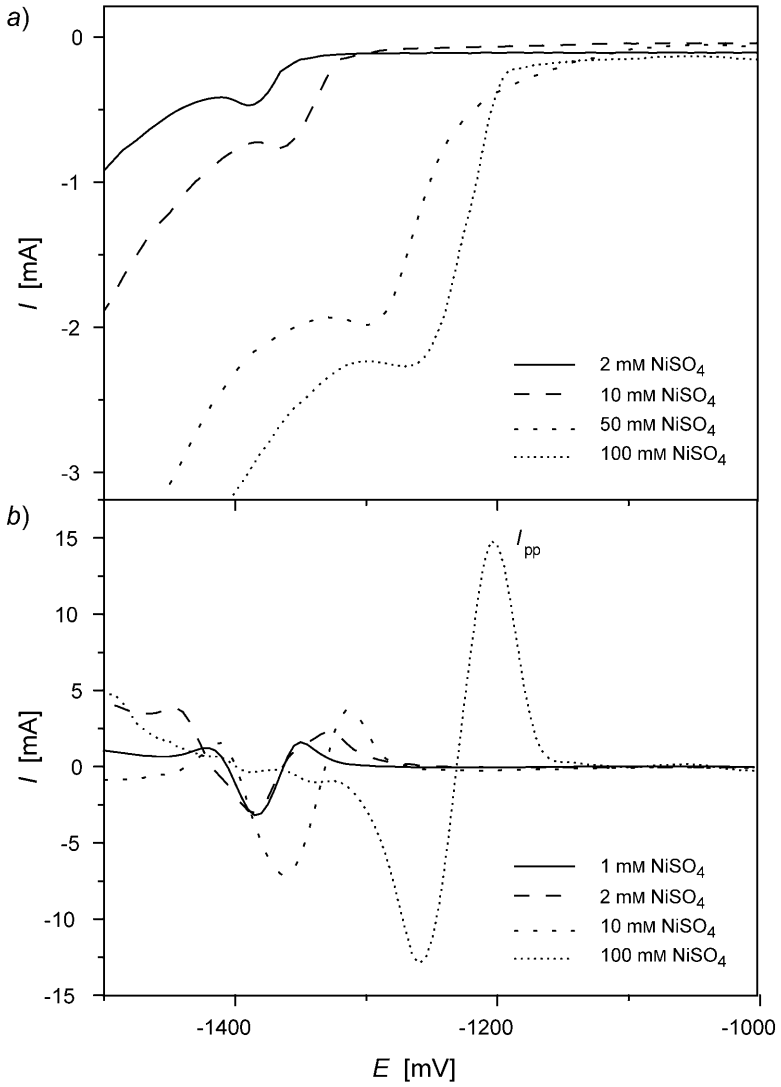

Fig. 6. a) *Cathodic cyclic voltammograms for nickel reduction on PIGE for various concentrations of* $NiSO_4$. Supporting electrolyte, 0.5M Na_2SO_4 (pH 4.0); scan rate, 25 mV/s; other experimental conditions as in *Fig. 1*. b) *Corresponding* E1 *and* E4 *elimination voltammograms*

low-hydrogen-content α-phase. It has been confirmed [25] that the hydrogen-permeation rate obtained during Ni plating in *Watts* electrolyte increases at the onset of the overall process, before reaching a steady-state value. This provides a possible rationalization for the two Ni-deposition peaks *A* and *B*, and, consequently, also for the two anodic peaks at -1530 mV (*Fig. 5*, *b*).

A different polarization behavior of Ni electrodeposition from sulfate supporting electrolyte was observed at pH 4 (*Fig. 6*, *a*). For all tested Ni^{2+} concentrations, one reduction signal was detected only, and the current maximum was shifted towards more-positive potentials with increasing Ni^{2+} concentration. It is quite reasonable to assume that the process becomes less complex on decreasing the concentration of H^+ in the electrolyte. The results of EVLS also provided less-complicated voltammograms (*Fig. 6*, *b*) than at pH 2. The elimination function *E4* reveals the kinetic effect

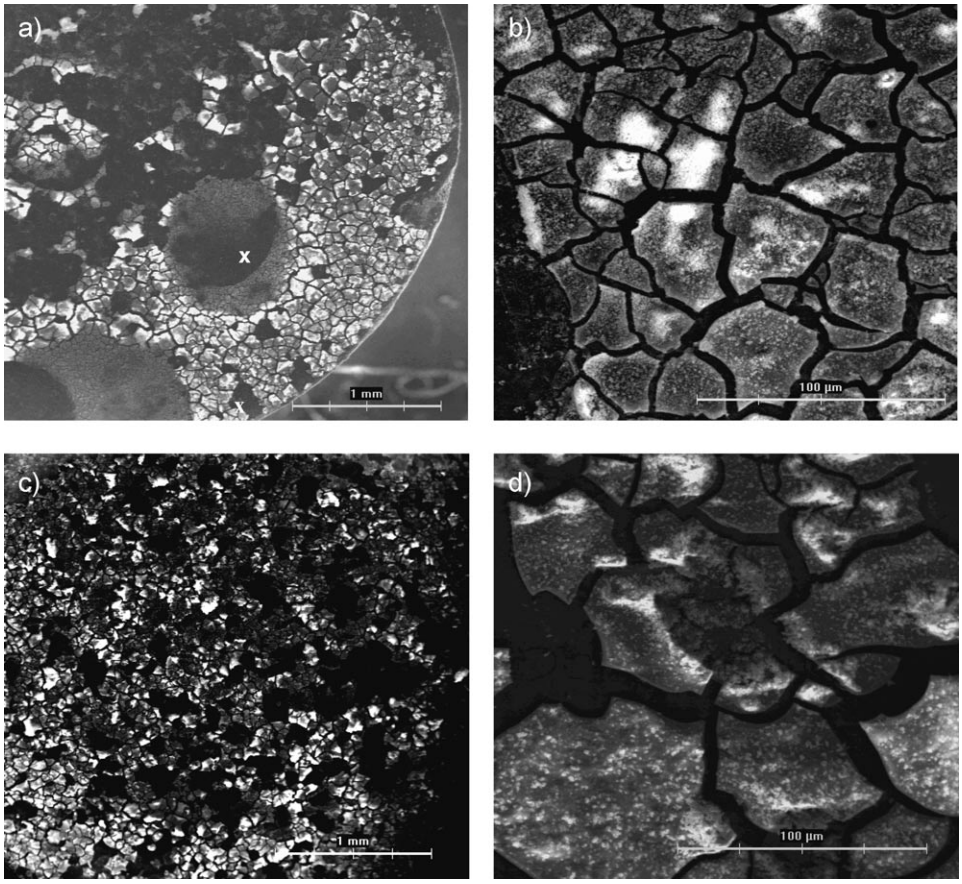

Fig. 7. *SEM Micrographs of nickel coatings deposited at different potentials and pH in 0.5*M *$NaSO_4$ containing 100 m*M *$NiSO_4$.* Conditions: *a*) -1362 mV, pH 2 (60-times magnified; *b*) detail of *a* (1000-times magnified; see mark in *a*); *c*) -1250 mV, pH 4 (60-times magnified); *d*) detail of *c* (1000-times magnified).

at the onset of the overall process and the diffusion control process at the maximum of the reduction signal. The degree of the kinetic effect expressed by the height of the peak (I_{pp}) indicates increasing hindrance of the electrode process with increasing Ni^{2+} concentration (see *Table*).

From an analytical point of view, it is worth noting that the remarkable increase of the peaks achieved by the elimination procedure facilitates the evaluation of measured voltammograms.

3. *Examination of Surface Morphology.* The surface morphology of PIGE and the deposited Ni films from different sulfate electrolytes was investigated by scanning electron microscopy (SEM). All deposited coatings were generated in potentiostatic regime for a deposition time of 10 min at selected potentials and at different pH values.

The character and appearance of the deposits were studied at higher Ni^{2+} concentration (100 mM). The surface morphology of the deposit obtained at -1362 mV (pH 2) is shown in (*Fig. 7*, *a* and *7*, *b*). As can be seen, the deposit is cracked, and not adhesive. The simultaneous H_2 reduction is evident from the dark circles sporadically created by H_2 bubbles growing on the electrode surface. The Ni deposit can also be observed under the arising bubbles, which indicates catalytic reduction of H_2 by deposited Ni. In the corresponding SEM micrographs recorded at pH 4 (*Fig. 7*, *c* and *7*, *d*), the destructive influence of H_2 was less pronounced.

Conclusion. – The electrodeposition of Ni from sulfate electrolyte has been investigated by voltammetric methods, complemented by SEM micrographs of the resulting deposit. With the aid of EVLS, the mechanisms of the process of H_2 and Ni reduction were discussed. Although EVLS could be applied to processes without mutual interactions of current components, in the present case, it enabled us to obtain the first information on the nature of these processes [18]. EVLS indicated kinetic control of the process at its onset, with a transition to diffusion control at more-negative potentials. This type of mechanism was corroborated by studying the anodic dissolution of the metal deposit obtained at different potentials, as well as by SEM micrographs.

In the Ni-containing electrolytes, the electrode process starts with H^+ reduction resulting in alkalization of the solution in the vicinity of the electrode, and formation of the electroactive particle $[NiOH]^+$. These two electrode processes were clearly detected at pH 2 and low Ni^{2+} concentration, and at high scan rates. Although the current at the peak potential is controlled by diffusion, the amount of deposited Ni is limited by surface coverage. Further, the SEM images showed the influence of H_2 evolution on the quality of the Ni deposit.

This research was supported by the *Czech-Slovak Cooperation* (Grant No. 046), the *Grant Agency of the Slovak Republic* (Grant No. 1/2118/05), the research project *INCHEMBIOL* (MSM 0021622412), and a project of the *Ministry of Education, Youth, and Sports* of the Czech Republic (No. 750/2005).

REFERENCES

[1] C. Q. Cui, Y. L. Jim, *Electrochim. Acta* **1995**, *40*, 1653.
[2] S. Z. Keith, J. Talbot, *J. Electochem. Soc.* **2000**, *147*, 189.
[3] P. Allongue, L. Cagnon, C. Gomes, A. Gundel, V. Costa, *Surf. Sci.* **2004**, *557*, 41.
[4] E. Gomez, R. Pollina, E. Valles, *J. Appl. Electrochem.* **1995**, *397*, 111.
[5] W. G. Proud, E. Gomez, E. Sarret, E. Valles, C. Muller, *J. Appl. Electrochem.* **1995**, *25*, 770.

[6] K. M. Yin, B. T. Lin, *Surf. Coat. Technol.* **1996**, *78*, 205.
[7] A. Brener, 'Electrodepostion of Alloys', Academic Press, New York, 1963.
[8] M. Šupicová, R. Rozik, L. Trnková, R. Oriňáková, M. Gálová, *J. Solid State Electrochem.* **2006**, *10*, 61.
[9] R. Oriňáková, M. Šupicová, L. Trnková, M. Gálová, *Electrochim. Acta* **2004**, *49*, 3587.
[10] J. I. Jinxing, C. W. Charles, *Electrochim. Acta* **1996**, *41*, 1549.
[11] B. V. Tilak, A. S. Gendorn, M. A. Mosoiu, *J. Appl. Electrochem.* **1977**, *7*, 495.
[12] H. Deligianni, L. T. Romankiw, *J. Res. Dev.* **1993**, *37*, 85.
[13] A. N. Correia, S. A. S. Machado, *Electrochim. Acta* **1998**, *43*, 367.
[14] O. Dračka, *J. Electroanal. Chem*. **1996**, *402*, 19.
[15] L. Trnková, O. Dračka, *J. Electroanal. Chem.* **1996**, *413*, 123.
[16] L. Trnková, R. Kizek, O. Dračka, *Electroanalysis* **2000**, *12*, 905.
[17] L. Trnková, J. Friml, O. Dračka, *Bioelectrochemistry* **2001**, *54*, 131.
[18] L. Trnková, *J. Electroanal. Chem.* **2005**, *582*, 258.
[19] A. J. Bard, L. R. Faulkner, 'Electrochemical Methods', 2nd edn., John Wiley & Sons, New York, 2001, p. 236.
[20] T. Erdey-Grúz, 'Kinetics of Electrode Processes', Akadémiai Kiadó, Budapest, 1972, p. 197.
[21] J. O. M. Bokris, E. C. Potter, *J. Chem. Phys.* **1952**, *20*, 614.
[22] J. Dvořák, J. Koryta, 'Electrochemie', Academia Praha, 1983, p. 324.
[23] A. Sabay-Reintjes, M. Fleischmann, *Electrochim. Acta* **1984**, *29*, 557.
[24] M. Fleischmann, A. Sabay-Reintjes, *Electrochim. Acta* **1984**, *29*, 69.
[25] L. Mirkova, G. Maurin, M. Monev, C. H. R. Tsvetkova, *J. Appl. Electrochem.* **2003**, *33*, 93.

Received November 28, 2005